

The Maximum T_c of Conventional Superconductors at Ambient Pressure

Kun Gao¹, Tiago F. T. Cerqueira², Antonio Sanna^{3,4}, Yue-Wen Fang⁵, Dorde Dangić^{5,6}, Ion Errea^{5,6,7}, Hai-Chen Wang¹, Silvana Botti¹ and Miguel A. L. Marques^{1,*}

¹*Research Center Future Energy Materials and Systems of the University Alliance Ruhr and Interdisciplinary Centre for Advanced Materials Simulation, Ruhr University Bochum, Universitätsstraße 150, D-44801 Bochum, Germany*

²*CFisUC, Department of Physics, University of Coimbra, Rua Larga, 3004-516 Coimbra, Portugal*

³*Max-Planck-Institut für Mikrostrukturphysik, Weinberg 2, D-06120 Halle, Germany*

⁴*Institut für Physik, Martin-Luther-Universität Halle-Wittenberg, D-06099 Halle, Germany*

⁵*Centro de Física de Materiales (CFM-MPC), CSIC-UPV/EHU, Manuel de Lardizabal Pasealekua 5, 20018 Donostia/San Sebastián, Spain*

⁶*Fisika Aplikatua Saila, University of the Basque Country (UPV/EHU), Europa Plaza 1, 20018 Donostia/San Sebastián, Spain*

⁷*Donostia International Physics Center (DIPC), Manuel de Lardizabal Pasealekua 4, 20018 Donostia/San Sebastián, Spain*

(Dated: February 26, 2025)

The theoretical maximum critical temperature (T_c) for conventional superconductors at ambient pressure remains a fundamental question in condensed matter physics. Through analysis of electron-phonon calculations for over 20 000 metals, we critically examine this question. We find that while hydride metals can exhibit maximum phonon frequencies of more than 5000 K, the crucial logarithmic average frequency ω_{\log} rarely exceeds 1800 K. Our data reveals an inherent trade-off between ω_{\log} and the electron-phonon coupling constant λ , suggesting that the optimal Eliashberg function that maximizes T_c is unphysical. Based on our calculations, we identify Li_2AgH_6 and its sibling Li_2AuH_6 as theoretical materials that likely approach the practical limit for conventional superconductivity at ambient pressure. Analysis of thermodynamic stability indicates that compounds with higher predicted T_c values are increasingly unstable, making their synthesis challenging. While fundamental physical laws do not strictly limit T_c to low-temperatures, our analysis suggests that achieving room-temperature conventional superconductivity at ambient pressure is extremely unlikely.

Since the groundbreaking discovery of superconductivity in mercury at 4.2 K in 1911 [1], superconductors have revolutionized both fundamental physics and technological applications. These materials have enabled transformative technologies including magnetic resonance imaging machines, magnetic levitation trains, and ultra-sensitive quantum devices such as SQUIDS. The quest for high-temperature superconductivity remains one of the grand challenges of solid-state physics, as raising the critical temperature would unlock unprecedented possibilities in power transmission, quantum computing, and particle acceleration.

Superconducting materials are traditionally divided into conventional and unconventional. In the former, the topic of the current work, the mechanism responsible for superconductivity is the electron-phonon interaction, electrons form Cooper pairs in a singlet state, and the energy gap has s-wave symmetry. These compounds are well understood within the Bardeen, Cooper, and Schrieffer (BCS) theory [2], or its strong coupling generalization, Eliashberg theory [3].

In the 1960s and 1970s, it was believed that the maximum T_c for conventional superconductors would likely be in the range of 30–40 K. This was based on the observed properties of known superconducting materials and the theoretical limits imposed by the electron-phonon interaction. The argument was that to achieve a higher T_c would require an unrealistically strong electron-phonon

coupling or an exceptionally high density of states, both of which seemed improbable given the materials known at the time. These beliefs were supported by experimental data. For example, elemental superconductors like Pb and Nb have $T_c = 7.2$ K and $T_c = 9.25$ K, respectively [4], while more complex compounds like Nb_3Sn or Nb_3Ge reach $T_c = 17.9$ K and $T_c = 21.8$ K respectively [5].

Currently, the compound with record conventional superconductivity at room pressure is MgB_2 , with a transition temperature of $T_c = 39$ K [6]. This compound exhibits two nearly noninteracting bands of different dimensionality [7], leading to the coexistence of two energy gaps in the same material [8]. The idea of multiple gaps coexisting in a single superconductor had been explored previously [9, 10], but MgB_2 stands out as the first system where this phenomenon is so prominently and distinctly manifested [11].

An alternative approach to achieving high-temperature superconductivity involves the chemical precompression of the hydrogen sub-lattice in hydrides materials [12]. This led to groundbreaking discoveries of very high- T_c superconductors, such as H_3S [13–15], LaH_{10} [16–19], YH_x [20–22], or even in ternary compounds such as LaBeH_8 , $(\text{La}, \text{Y})\text{H}_{10}$, $(\text{La}, \text{Ce})\text{H}_9$, etc. [23–28]. Unfortunately, all these systems require very high pressures, seriously limiting their application to technology.

A key question in this field is what is the upper limit to the critical temperature of superconductors [29–31]. Based on the observation that the coupling constant depends mainly on the phonon frequencies, McMillan in

* miguel.marques@rub.de

1968 [32] already derived an approximate expression of T_c^{\max} . His result, however, only holds for a *given class of materials* and therefore does not provide an absolute value for this quantity. Further insight can be obtained by maximizing T_c given by McMillan's formula

$$T_c^{\text{McMillan}} = \frac{\omega_{\log}}{1.20} \exp\left(-1.04 \frac{1 + \lambda}{\lambda - \mu^*(1 + 0.62\lambda)}\right), \quad (1)$$

where μ^* is the Coulomb pseudopotential, λ is the electron-phonon coupling constant

$$\lambda = 2 \int_0^{+\infty} \frac{\alpha^2 F(\omega)}{\omega} d\omega \quad (2)$$

and $\alpha^2 F(\omega)$ is the Eliashberg spectral function, calculated from the electron-phonon coupling matrix elements. With ω_{\log} we indicate the logarithmic average of the phonon frequencies:

$$\omega_{\log} = \exp\left[\frac{\lambda}{2} \int_0^{+\infty} \ln(\omega) \frac{\alpha^2 F(\omega)}{\omega} d\omega\right]. \quad (3)$$

By setting, for simplicity, the Coulomb pseudopotential μ^* to zero, one obtains that the maximum is attained at $\lambda \approx 2$. However, McMillan's formula is only valid for values of $\lambda \lesssim 1.5$, while no maximum value for T_c exists in the original Eliashberg theory [29]. It is also frequently argued that the value of λ is limited, as the lattice becomes eventually unstable for very large values of the coupling constant. However, there are some experimentally known superconductors with very high values of λ , well above 2.0, both at ambient (such as Pb-Bi compounds [33]) and under pressure [34].

Recent works estimated the maximum T_c of conventional superconductivity from fundamental limits [35–37]. They all agree on a value of 300–600 K at ambient pressure, suggesting that superconductors may exist at ambient temperature. In the following, we critically look at the basic assumptions used in these estimates. This is done by analyzing experimentally-known superconductors and our calculations of the electron-phonon interaction and superconducting properties for more than 20 000 metals [38, 39]. This is by far the largest dataset available to date with calculated superconducting properties, and it includes metals with a large variety of chemical elements and crystal structures. Although it is not comprehensive, it is rather extensive, giving us a very good overview of conventional superconductivity in materials space.

The first step is to determine what is the largest phonon frequency ω_{\max} that one can reasonably expect in a realistic compound. Reference 37 derived the expression

$$\omega_{\max} = \frac{E^{\text{electronic}}}{\sqrt{m}}, \quad (4)$$

where $E^{\text{electronic}}$ is a typical electronic energy, and m is an atomic mass. By inserting a typical $E^{\text{electronic}} = 1$ Ry,

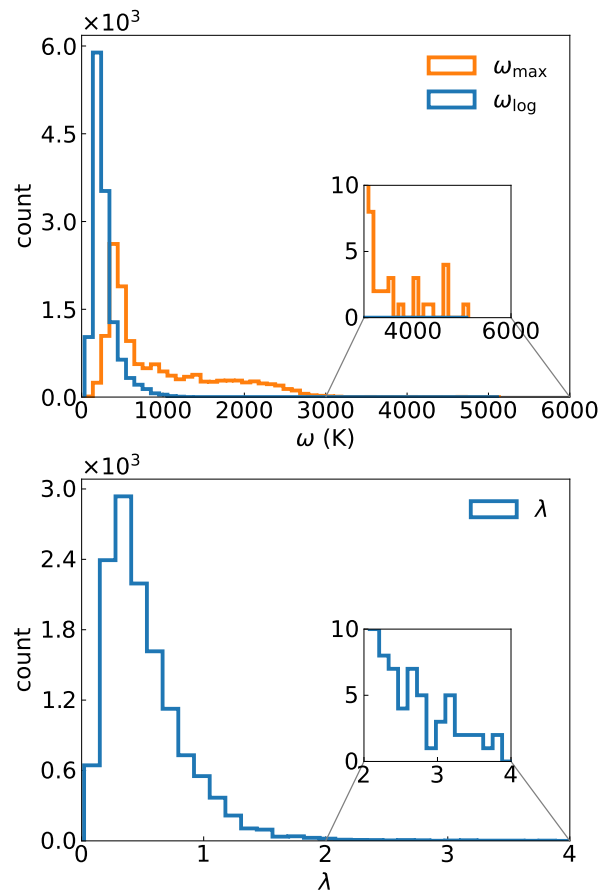


FIG. 1. Histogram of (top) the maxima (ω_{\max}) and logarithmic average (ω_{\log}) of phonon frequencies and (bottom) the electron-phonon coupling constants (λ) calculated for around 20 000 metals (see Refs. [38]).

and the proton mass $m = m^{\text{proton}}$ into the formula, they obtained $\omega_{\max} = 3680$ K. Compared to the vibrational frequency of H_2 that is almost 6000 K [40], this value does not appear to be an overestimation.

The same conclusion can be reached by looking at the calculated values for our materials depicted in fig. 1. The distribution of values of ω_{\max} exhibits two maxima, one at around 500 K and another around 2000 K. Although the overwhelming majority of the compounds have ω_{\max} below 3000 K, we find a few that extend to 5400 K, well beyond the estimation of Ref. 37. Not surprisingly, all of these are hydrides. An example of one such material, with a calculated $\omega_{\max} = 5396$ K, is the hypothetical AgTl_2H_2 . This is a compound that contains isolated H_2 molecules inside a AgTl_2 framework (see Supplementary Information, SI). The H–H distance is 0.78 Å, only slightly larger than the value of 0.76 Å in solid hydrogen calculated in the same approximation. As expected by the extreme difference of masses, the phonon band structure splits into separated manifolds, with the lowest lying states with Tl and Ag character and the highest states coming from H. The H_2 stretching mode has negli-

gible dispersion, and can be found at around 5400 K. The Ag–Ti and lowest lying H-modes all couple very strongly to the electrons, leading to the large $\lambda = 1.1$ (and a $T_c \sim 11.5$ K). As expected by the very high frequency, the highest lying phonon mode has a negligible contribution to λ , even if $\alpha^2F(\omega)$ exhibits a very high peak at that frequency.

In fig. 1 we also plot the distribution of the values of ω_{\log} . Contrary to ω_{\max} , ω_{\log} has a single peak at very low frequency, and decays rapidly with frequency. At the end of the tail, at ω_{\log} values in excess of 1800 K we find a few hydrides, such as the hypothetical perovskite NaNiH_3 , and some ordered crystals of boron-doped sp^3 carbon (see SI). In the case of the hydride, only the high frequency H-modes have a significant coupling to the electrons, leading to a large logarithmic average but a very small value of λ and consequently of T_c . The boron-doped case takes advantage of the high-energy of the carbon modes (due to the very strong C–C sp^3 bond) and from the fact that phonon modes couple strongly to the electrons in a large energy range. As expected, also in this case λ has moderate values, of the order of 0.5–0.6, leading to T_c in the range of 10–30 K.

As the determinant factor for the calculation of T_c is ω_{\log} and not ω_{\max} , from this discussion it seems much more reasonable to use values of the order of 1800 K, and not $\omega_{\max} = 3680$ K, as in Ref. 37.

The next step in the estimation of the maximum value of T_c is the optimization of the shape of $\alpha^2F(\omega)$, assuming a maximum phonon frequency of ω_{\max} . A free optimization of this function would obviously lead to $T_c = \infty$, as $\alpha^2F(\omega)$ is not constrained by any sum-rule. Therefore, Trachenko *et al.* fixed $\lambda = 2$ [37], the value that maximizes T_c according to McMillan’s formula. From the considerations above, and from the lower panel of fig. 1, $\lambda = 2$ seems to be a reasonable value, perfectly reachable in a variety of compounds. The hypothetical compounds we have in our dataset with highest values of $\lambda \approx 3.3$ are ClB_2C_8 and Al_2OsH_7 (see SI). The former is a C clathrate p-doped with B and co-doped with endohedral Cl, with a $\omega_{\log} = 425$ K and a calculated $T_c = 55$ K. The latter, that exhibits a Al_2Os framework that includes a large quantity of hydrogen, has an ω_{\log} of almost 300 K, leading to $T_c = 38$ K.

The optimal shape of $\alpha^2F(\omega)$ obtained by Ref. 37 by optimizing the T_c calculated from the Eliashberg equations is a narrow peak at ω_{\max} . Actually, the same conclusion follows directly from McMillan’s formula for T_c . For a fixed value of λ , the value of T_c changes linearly with ω_{\log} . In turn, the maximum value of ω_{\log} is obtained when $\alpha^2F(\omega) \sim \delta(\omega - \omega_{\max})$, leading to $\omega_{\log} = \omega_{\max}$. If, for the sake of the argument, we insert $\lambda = 2$, $\omega_{\log} = 1800$ K into the McMillan function, and assume a value of $\mu^* = 0.1$, we obtain $T_c = 260$ K. This is smaller than the value of Ref. 37, but still much larger than the current record of MgB_2 .

It is most likely, however, that this limit is unattainable for any physical system at ambient pressure. In fact,

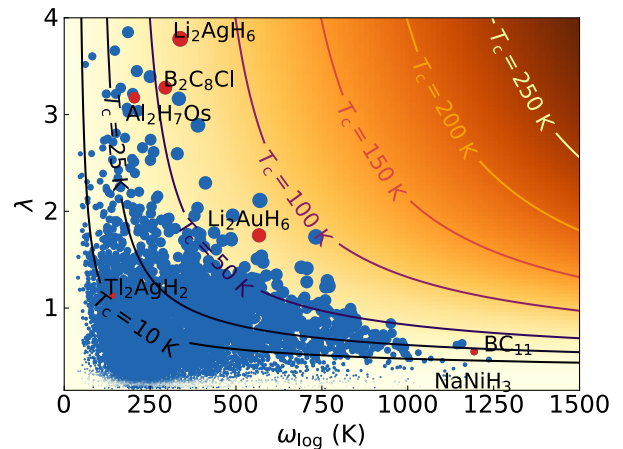


FIG. 2. Scatter plot of ω_{\log} versus λ for all calculated systems, the contour lines are T_c from McMillan’s formula with $\mu^* = 0.1$.

the parameters ω_{\log} and λ are not entirely independent, as they are two different moments of the same $\alpha^2F(\omega)$ function. This was already recognized in the seminal work of McMillan in 1968 [32], where it was recognized that the most important dependence of λ is on an average phonon frequency. Obviously ω_{\log} is favored by high frequencies, while λ by low frequencies, so the shape of the optimal $\alpha^2F(\omega)$ that maximizes T_c (and that only contains a *single*, very high-frequency, flat-band phonon mode that couples very strongly to the electrons) seems to be unattainable physically.

This evidence is also supported by the data depicted in fig. 2, where we plot the relationship between ω_{\log} and λ for all compounds in our dataset. The size of the circles is proportional to T_c and in the background we plot the contour lines of constant T_c as calculated from McMillan’s formula with $\mu^* = 0.1$. We see that, as expected, compounds with very large values of ω_{\log} often have small λ and vice-versa. Furthermore, no material comes close to the optimal case, and compounds with the highest values of T_c are the ones that achieve a good compromise between reasonable high ω_{\log} and λ .

As an example, we will look at the compounds with the highest T_c in our dataset, specifically Li_2AgH_6 and Li_2AuH_6 (see fig. 3 and SI). These compound crystallize in the same cubic structure as Mg_2IrH_6 , Mg_2PdH_6 , Mg_2PtH_6 , etc. that were recently proposed [41, 42] as high- T_c superconductors. Both materials are thermodynamically unstable at ambient pressure at respectively 0.319 eV/atom and 0.172 eV/atom above the convex hull for the Ag and the Au compounds, and are not significantly stabilized by pressure (at least up to 50 GPa, see SI).

The electronic band structure of Li_2AgH_6 resembles the one of Mg_2IrH_6 , with a single band crossing the Fermi surface. This band, with very strong H-character, is however more dispersive in the present case. Also the phonon

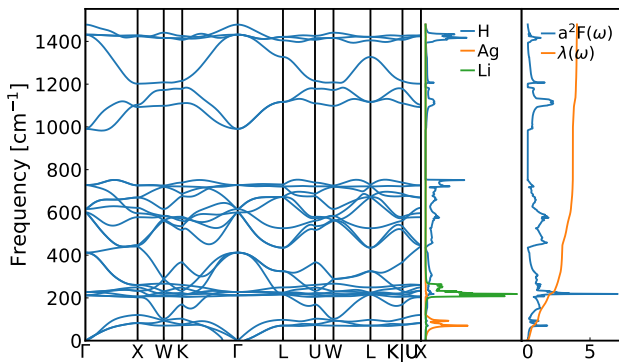


FIG. 3. Harmonic phonon band structure, density of phonon states, and Eliashberg spectral function $\alpha^2 F(\omega)$ of Li_2AgH_6 calculated within the harmonic approximation.

band structure is similar, with the acoustic modes mostly composed by vibrations of the heavier atom, followed by modes stemming from the alkali or alkaline earth metal. Finally, there are three separate manifolds of phonon bands. In Li_2AgH_6 the lowest manifold contains both H and Li character due to the small difference between the atomic masses of these elements. Essentially all modes contribute to the very high value of $\lambda \approx 4$.

We would like to note that one of the acoustic phonon branches exhibits (small) imaginary values close to the Γ . This is a shortcoming of the harmonic approximation, and the structure is perfectly dynamically stable when anharmonic and quantum nuclear effects are taken into account (see SI) [43, 44]. In any case, 95% of the electron-phonon coupling comes from mid-low frequency modes which are almost identical between harmonic and anharmonic calculations.

In order to obtain a more accurate T_c estimation within modern superconductivity methods we have recomputed the value of T_c using two state-of-the-art approaches which, unlike more conventional methods, include the electron-phonon coupling and the Coulomb interaction calculated from first-principles. These are the full Eliashberg approach of Ref. 45 and density functional theory for superconductors [46–50] (SCDFT). For the sake of these high-accuracy calculations the electron-phonon coupling was recomputed using a Monte-Carlo k -mesh accumulated on the Fermi surface, on which the electron-phonon matrix elements are linearly interpolated [51]. This ensures a perfect convergence of the nesting properties entering the definition of the Eliashberg spectral function.

The resulting critical temperature for Li_2AhH_6 is 108.8 K in Eliashberg theory and 83.0 K in SCDFT. Although both approaches are derived from the Migdal approximation for the electron-phonon self energy [52] and assume a static Coulomb interaction, the slightly different T_c prediction is dictated by the approximation chain that leads to each computational scheme. On one hand, in SCDFT there is the approximation to the anomalous exchange-correlation functional [47], which adds addi-

tional approximations to the form of the self-energy. On the other hand, in Eliashberg theory the energy dependence of the Coulomb interaction is neglected at the scale of the phononic energies. However, considering that the electron-phonon coupling parameter λ is very high, the functional approximation of SCDFT might be slightly beyond its validity range [47]. Therefore we expect that, in this case, the Eliashberg estimation should be more accurate.

It is interesting that the Eliashberg estimation of T_c is in very good agreement with the one obtained by means of the McMillan-Allen-Dynes approach using a standard $\mu^* = 0.1$. This indicates that Coulomb interactions act as expected for a conventional sp-system [53]. This differs from what is observed in Mg_2IrH_6 which, as discussed in Ref. 41, has its T_c overestimated by the μ^* model [54]. The reason is the presence of a peak in the density of states at the Fermi level, that is close to a large band gap, leading to a poor Coulomb renormalization [53, 55]. The Li_2AgH_6 system also features a peak in the density-of-states and a band gap, however the peak is broader, while the band gap is very small, leading to an overall smoother density profile and efficient Coulomb renormalization.

A similar analysis can be extended to Li_2AuH_6 . This system has electronic, phononic and superconducting properties nearly identical to its Ag twin. The predicted superconducting T_c including Coulomb interactions is 91.0 K and 116.1 K in SCDFT and Eliashberg, respectively.

In view of the discussion before, these materials seem to be ideal cases for conventional superconductivity, and their T_c is likely in the maximum range of what can be achievable at ambient pressure. We note that these are isotropic superconductors, where the effect of anisotropy accounts for less than 1% of the value of T_c . This is the opposite of MgB_2 , where the electron-phonon coupling mostly acts on the σ bands, and an isotropic calculations leads to an underestimation of T_c by almost a factor of two. The isotropic superconducting state of Li_2AgH_6 or Li_2AuH_6 , if experimentally realized, would not only have a critical temperature above liquid nitrogen, but it would also be more suitable for high-field applications. In fact these applications require impurities and defects to work as pinning centers for magnetic flux lines and reduce the Ginsburg-Landau coherence-length. Isotropic superconductors are more likely to be stable upon the introduction of crystalline defects and still be affected by their scattering potential.

Finally, we would like to discuss the issue of synthesizability. Most of the compounds discussed above, and others that have been proposed in the literature, with high- T_c are hypothetical, and up to now none has been stabilized at ambient pressure. To better understand this problem, we plot in fig. 4 the distance to the convex hull of thermodynamic stability and the calculated transition temperature of all compounds in our dataset. We also indicate the Pareto front that corresponds to this data. The values of T_c are obtained with an isotropic theory, so

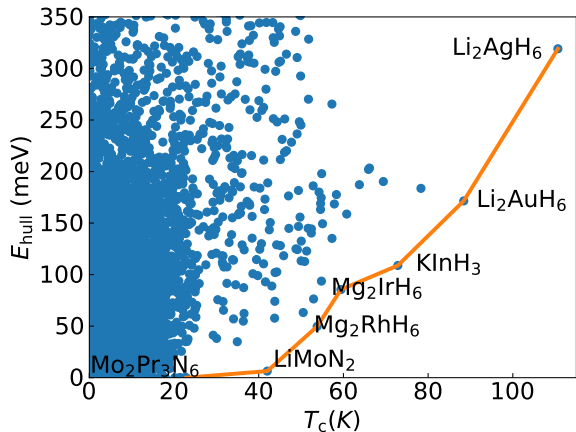


FIG. 4. Scatter plot of the distance to the convex hull of stability versus the superconducting transition temperature for all compounds in our dataset. In orange we also indicate the Pareto front corresponding to this data. Compounds on the Pareto front are labeled.

the transition temperature of MgB_2 is considerably underestimated. We also note that although being close to the hull is not a synonym of synthesizability, the higher the distance to the hull for a given compound, the smaller the probability that this compound can be stabilized experimentally.

Very close to the hull, we find that the compound with highest predicted T_c is LiMoN_2 with around 40 K [39]. Unfortunately, this compound exhibits intrinsic defects that lower the high density of states at the Fermi level and destroy superconductivity [39, 56]. If it is possible to resolve this problem experimentally and synthesize the pristine compound is at this point unknown [57]. At higher values of T_c we find several hydrides and boron-carbides. Unfortunately, all these compounds are unstable thermodynamically with a distance to the hull that increases rapidly along the Pareto front. This is easy to understand as hydrides prefer charge-compensated, semi-conducting (or insulating) phases and are therefore destabilized in the metallic phase, and boron induces stresses in the very strong diamond framework increasing its energy. A possible path through the high-pressure synthesis followed by quenching of these compounds to ambient pressure is commonly suggested in the literature [58–60], however it is still unproved to this date, and remains highly speculative.

In summary, by analyzing data from more than 20 000 electron-phonon calculations we critically discussed the possible maximum T_c of conventional superconductors at ambient pressure. It seems clear that it is possible to design hypothetical compound with values of T_c reaching 100–120 K, much larger than the current experimental record, but still very far from room temperature. Unfortunately, all compounds with high T_c appear to be thermodynamically unstable, raising questions about their experimental synthesis and characterization. It is true that physical laws do not restrict T_c to go beyond 100–120 K, but in practice our data show that the experimental realization of a compound with such high T_c is extremely unlikely.

ACKNOWLEDGEMENTS

This work was supported by Simons Foundation through the Collaboration on New Frontiers in Superconductivity (Grant No. SFI-MPS-NFS-00006741-10) and by the Keele foundation. T.F.T.C acknowledges financial support from FCT - Fundação para a Ciência e Tecnologia, I.P. through the project CEECINST/00152/2018/CP1570/CT0006 with DOI identifier 10.54499/CEECINST/00152/2018/CP1570/CT0006, and computing resources provided by the project Advanced Computing Project 2023.14294.CPCA.A3, platform Deucalion. H.-C.W and M.A.L.M acknowledge the computing time on the high-performance computer Noctua 2 at the NHR Center PC2. Y.-W.F., Đ.D., and I.E. acknowledge funding from the European Research Council (ERC) under the European Union’s Horizon 2020 research and innovation program (grant agreement No. 802533) as well as EuroHPC for granting the access to Lumi located in CSC’s data center in Kajaani, Finland, (Project ID EHPC-REG-2024R01-084) and the technical and human support provided by DIPC Supercomputing Center. I.E. also received funding the Spanish Ministry of Science and Innovation (Grant No. PID2022-142861NA-I00), and the Department of Education, Universities and Research of the Eusko Jaurlaritza and the University of the Basque Country UPV/EHU (Grant No. IT1527-22). K.G. acknowledges financial support from the China Scholarship Council. The authors acknowledge enlightening discussions with the partners of the SuperC collaboration.

-
- [1] H. K. Onnes, The superconductivity of mercury, *Comm. Phys. Lab. Univ. Leiden* **122**, 124 (1911).
 [2] J. Bardeen, L. N. Cooper, and J. R. Schrieffer, Microscopic theory of superconductivity, *Phys. Rev.* **106**, 162 (1957).
 [3] G. M. Eliashberg, Interactions between electrons and lattice vibrations in a superconductor, *Sov. Phys. JETPL*

- 11**, 696 (1960).
 [4] C. Buzea and K. Robbie, Assembling the puzzle of superconducting elements: a review, *Supercond. Sci. Technol.* **18**, R1 (2004).
 [5] G. R. Stewart, Superconductivity in the A15 structure, *Physica C* **514**, 28 (2015).

- [6] J. Nagamatsu, N. Nakagawa, T. Muranaka, Y. Zenitani, and J. Akimitsu, Superconductivity at 39 K in magnesium diboride, *Nature* **410**, 63 (2001).
- [7] P. C. Canfield and G. W. Crabtree, Magnesium diboride: Better late than never, *Phys. Today* **56**, 34–40 (2003).
- [8] A. Y. Liu, I. Mazin, and J. Kortus, Beyond eliasberg superconductivity in MgB₂: anharmonicity, two-phonon scattering, and multiple gaps, *Phys. Rev. Lett.* **87**, 087005 (2001).
- [9] H. Suhl, B. T. Matthias, and L. R. Walker, Bardeen-cooper-schrieffer theory of superconductivity in the case of overlapping bands, *Phys. Rev. Lett.* **3**, 552 (1959).
- [10] G. Binnig, A. Baratoff, H. Hoenig, and J. Bednorz, Two-band superconductivity in Nb-doped SrTiO₃, *Phys. Rev. Lett.* **45**, 1352 (1980).
- [11] H. J. Choi, D. Roundy, H. Sun, M. L. Cohen, and S. G. Louie, The origin of the anomalous superconducting properties of MgB₂, *Nature* **418**, 758 (2002).
- [12] J. A. Flores-Livas, L. Boeri, A. Sanna, G. Profeta, R. Arita, and M. Eremets, A perspective on conventional high-temperature superconductors at high pressure: Methods and materials, *Phys. Rep.* **856**, 1 (2020).
- [13] Y. Li, J. Hao, H. Liu, Y. Li, and Y. Ma, The metallization and superconductivity of dense hydrogen sulfide, *J. Chem. Phys.* **140**, 174712 (2014).
- [14] D. Duan, Y. Liu, F. Tian, D. Li, X. Huang, Z. Zhao, H. Yu, B. Liu, W. Tian, and T. Cui, Pressure-induced metallization of dense (H₂S)₂H₂ with high- T_c superconductivity, *Sci. Rep.* **4**, 6968 (2014).
- [15] A. Drozdov, M. Eremets, I. Troyan, V. Ksenofontov, and S. I. Shylin, Conventional superconductivity at 203 kelvin at high pressures in the sulfur hydride system, *Nature* **525**, 73 (2015).
- [16] H. Liu, I. I. Naumov, R. Hoffmann, N. Ashcroft, and R. J. Hemley, Potential high- T_c superconducting lanthanum and yttrium hydrides at high pressure, *Proc. Natl. Acad. Sci.* **114**, 6990 (2017).
- [17] F. Peng, Y. Sun, C. J. Pickard, R. J. Needs, Q. Wu, and Y. Ma, Hydrogen clathrate structures in rare earth hydrides at high pressures: possible route to room-temperature superconductivity, *Phys. Rev. Lett.* **119**, 107001 (2017).
- [18] A. Drozdov, P. Kong, V. Minkov, S. Besedin, M. Kuzovnikov, S. Mozaffari, L. Balicas, F. Balakirev, D. Graf, V. Prakapenka, *et al.*, Superconductivity at 250 K in lanthanum hydride under high pressures, *Nature* **569**, 528 (2019).
- [19] M. Somayazulu, M. Ahart, A. K. Mishra, Z. M. Geballe, M. Baldini, Y. Meng, V. V. Struzhkin, and R. J. Hemley, Evidence for superconductivity above 260 K in lanthanum superhydride at megabar pressures, *Phys. Rev. Lett.* **122**, 027001 (2019).
- [20] Y. Li, J. Hao, H. Liu, S. T. John, Y. Wang, and Y. Ma, Pressure-stabilized superconductive yttrium hydrides, *Sci. Rep.* **5**, 9948 (2015).
- [21] P. Kong, V. S. Minkov, M. A. Kuzovnikov, A. P. Drozdov, S. P. Besedin, S. Mozaffari, L. Balicas, F. F. Balakirev, V. B. Prakapenka, S. Chariton, *et al.*, Superconductivity up to 243 K in the yttrium-hydrogen system under high pressure, *Nat. Commun.* **12**, 5075 (2021).
- [22] I. A. Troyan, D. V. Semenov, A. G. Kvashnin, A. V. Sadakov, O. A. Sobolevskiy, V. M. Pudalov, A. G. Ivanova, V. B. Prakapenka, E. Greenberg, A. G. Gavriliuk, *et al.*, Anomalous high-temperature superconductivity in YH₆, *Adv. Mater.* **33**, 2006832 (2021).
- [23] P. Song, Z. Hou, K. Nakano, K. Hongo, and R. Maezono, Potential high- T_c superconductivity in YCeH_x and LaCeH_x under pressure, *Mater. Today Phys.* **28**, 100873 (2022).
- [24] D. V. Semenov, I. A. Troyan, A. G. Ivanova, A. G. Kvashnin, I. A. Kruglov, M. Hanfland, A. V. Sadakov, O. A. Sobolevskiy, K. S. Pervakov, I. S. Lyubutin, *et al.*, Superconductivity at 253 K in lanthanum-yttrium ternary hydrides, *Mater. Today* **48**, 18 (2021).
- [25] Y. Song, J. Bi, Y. Nakamoto, K. Shimizu, H. Liu, B. Zou, G. Liu, H. Wang, and Y. Ma, Stoichiometric ternary superhydride LaBeH₈ as a new template for high-temperature superconductivity at 110 K under 80 GPa, *Phys. Rev. Lett.* **130**, 266001 (2023).
- [26] J. Bi, Y. Nakamoto, P. Zhang, K. Shimizu, B. Zou, H. Liu, M. Zhou, G. Liu, H. Wang, and Y. Ma, Giant enhancement of superconducting critical temperature in substitutional alloy (La,Ce)H₉, *Nat. Commun.* **13**, 5952 (2022).
- [27] W. Chen, X. Huang, D. V. Semenov, S. Chen, D. Zhou, K. Zhang, A. R. Oganov, and T. Cui, Enhancement of superconducting properties in the La-Ce-H system at moderate pressures, *Nat. Commun.* **14**, 2660 (2023).
- [28] D. V. Semenov, I. A. Troyan, A. V. Sadakov, D. Zhou, M. Galasso, A. G. Kvashnin, A. G. Ivanova, I. A. Kruglov, A. A. Bykov, K. Y. Terent'ev, *et al.*, Effect of magnetic impurities on superconductivity in LaH₁₀, *Adv. Mater.* **34**, 2204038 (2022).
- [29] L. P. Gor'kov and V. Z. Kresin, Colloquium: High pressure and road to room temperature superconductivity, *Rev. Mod. Phys.* **90**, 011001 (2018).
- [30] L. Boeri and G. B. Bachelet, Viewpoint: the road to room-temperature conventional superconductivity, *J. Phys.: Condens. Matter* **31**, 234002 (2019).
- [31] L. Boeri, R. G. Hennig, P. J. Hirschfeld, G. Profeta, A. Sanna, E. Zurek, W. E. Pickett, M. Amsler, R. Dias, M. Eremets, C. Heil, R. Hemley, H. Liu, Y. Ma, C. Pierleoni, A. Kolmogorov, N. Rybin, D. Novoselov, V. I. Anisimov, A. R. Oganov, C. J. Pickard, T. Bi, R. Arita, I. Errea, C. Pellegrini, R. Requist, E. Gross, E. R. Margine, S. R. Xie, y. quan, a. hire, L. Fanfarillo, G. R. Stewart, J. J. Hamlin, V. Stanev, R. S. Gonnelli, E. Pizzati, D. Romanin, D. Daghero, and R. Valenti, The 2021 room-temperature superconductivity roadmap, *J. Phys.: Condens. Matter* **33**, 0 (2021).
- [32] W. McMillan, Transition temperature of strong-coupled superconductors, *Phys. Rev.* **167**, 331 (1968).
- [33] T. Chen, J. Leslie, and H. Smith, Electron tunneling study of amorphous Pb-Bi superconducting alloys, *Physica* **55**, 439 (1971).
- [34] K. Tanaka, J. Tse, and H. Liu, Electron-phonon coupling mechanisms for hydrogen-rich metals at high pressure, *Phys. Rev. B* **96**, 100502 (2017).
- [35] D. V. Semenov, B. L. Altshuler, and E. A. Yuzbashyan, Fundamental limits on the electron-phonon coupling and superconducting T_c , arXiv [10.48550/ARXIV.2407.12922](https://arxiv.org/abs/10.48550/ARXIV.2407.12922) (2024).
- [36] M. V. Sadovskii, Upper limit for the superconducting transition temperature in eliasberg-mcmillan theory, *JETP Lett.* **120**, 205–207 (2024).
- [37] K. Trachenko, B. Monserrat, M. Hutcheon, and C. J. Pickard, Upper bounds on the highest phonon frequency and superconducting temperature from fundamental

- physical constants, arXiv [10.48550/ARXIV.2406.08129](https://arxiv.org/abs/10.48550/ARXIV.2406.08129) (2024).
- [38] T. F. T. Cerqueira, Y.-W. Fang, I. Errea, A. Sanna, and M. A. L. Marques, Searching materials space for hydride superconductors at ambient pressure, *Adv. Funct. Mater.* **34**, 2404043 (2024).
- [39] T. F. Cerqueira, A. Sanna, and M. A. Marques, Sampling the materials space for conventional superconducting compounds, *Adv. Mater.* **36**, 2307085 (2024).
- [40] K. P. Huber and G. Herzberg, *Molecular Spectra and Molecular Structure* (Springer US, 1979).
- [41] A. Sanna, T. F. T. Cerqueira, Y.-W. Fang, I. Errea, A. Ludwig, and M. A. L. Marques, Prediction of ambient pressure conventional superconductivity above 80 K in hydride compounds, *npj Comput. Mater.* **10**, 44 (2024).
- [42] M. F. Hansen, L. J. Conway, K. Dolui, C. Heil, C. J. Pickard, A. Pakhomova, M. Mezouar, M. Kunz, R. P. Prasankumar, and T. A. Strobel, Synthesis of Mg_2IrH_5 : A potential pathway to high- T_c hydride superconductivity at ambient pressure, *Phys. Rev. B* **110**, 214513 (2024).
- [43] I. Errea, M. Calandra, and F. Mauri, Anharmonic free energies and phonon dispersions from the stochastic self-consistent harmonic approximation: Application to platinum and palladium hydrides, *Phys. Rev. B* **89**, 064302 (2014).
- [44] L. Monacelli, R. Bianco, M. Cherubini, M. Calandra, I. Errea, and F. Mauri, The stochastic self-consistent harmonic approximation: calculating vibrational properties of materials with full quantum and anharmonic effects, *J. Phys. Condens. Matter.* **33**, 363001 (2021).
- [45] C. Pellegrini, R. Heid, and A. Sanna, Eliashberg theory with ab-initio coulomb interactions: a minimal numerical scheme applied to layered superconductors, *J. Phys.: Mater.* **5**, 024007 (2022).
- [46] C. Pellegrini and A. Sanna, Ab initio methods for superconductivity, *Nat. Rev. Phys.* **6**, 509 (2024).
- [47] A. Sanna, C. Pellegrini, and E. K. U. Gross, Combining Eliashberg theory with density functional theory for the accurate prediction of superconducting transition temperatures and gap functions, *Phys. Rev. Lett.* **125**, 057001 (2020).
- [48] L. N. Oliveira, E. K. U. Gross, and W. Kohn, Density-functional theory for superconductors, *Phys. Rev. Lett.* **60**, 2430 (1988).
- [49] M. Lüders, M. A. L. Marques, N. N. Lathiotakis, A. Floris, G. Profeta, L. Fast, A. Continenza, S. Massidda, and E. K. U. Gross, Ab initio theory of superconductivity. i. density functional formalism and approximate functionals, *Phys. Rev. B* **72**, 024545 (2005).
- [50] M. A. L. Marques, M. Lüders, N. N. Lathiotakis, G. Profeta, A. Floris, L. Fast, A. Continenza, E. K. U. Gross, and S. Massidda, Ab initio theory of superconductivity. ii. application to elemental metals, *Phys. Rev. B* **72**, 024546 (2005).
- [51] A. Sanna, C. Pellegrini, E. Liebhaber, K. Rossnagel, K. J. Franke, and E. K. U. Gross, Real-space anisotropy of the superconducting gap in the charge-density wave material 2H-NbSe_2 , *npj Quantum Mater.* **7**, 6 (2022).
- [52] A. B. Migdal, Interaction between electrons and lattice vibrations in a normal metal, *Sov. Phys. JETPL* **34**, 996 (1958).
- [53] P. B. Allen and B. Mitrović, Theory of superconducting T_c , in *Solid State Physics* (Elsevier, 1983) p. 1–92.
- [54] P. Morel and P. W. Anderson, Calculation of the superconducting state parameters with retarded electron-phonon interaction, *Phys. Rev.* **125**, 1263 (1962).
- [55] D. J. Scalapino, J. R. Schrieffer, and J. W. Wilkins, Strong-coupling superconductivity. I, *Phys. Rev.* **148**, 263 (1966).
- [56] S. H. Elder, L. H. Doerr, F. J. DiSalvo, J. B. Parise, D. Guyomard, and J. M. Tarascon, Lithium molybdenum nitride (LiMoN_2): the first metallic layered nitride, *Chem. Mater.* **4**, 928–937 (1992).
- [57] S. M. Hunter, *A structural and reactivity study of lithium molybdenum nitride*, Ph.D. thesis, University of Glasgow (2008).
- [58] K. P. Hilleke and E. Zurek, Tuning chemical precompression: Theoretical design and crystal chemistry of novel hydrides in the quest for warm and light superconductivity at ambient pressures, *J. Appl. Phys.* **131**, 070901 (2022).
- [59] R. Lucrezi, S. Di Cataldo, W. von der Linden, L. Boeri, and C. Heil, In-silico synthesis of lowest-pressure high- T_c ternary superhydrides, *npj Comput. Mater.* **8**, 119 (2022).
- [60] Đ. Dangić, Y.-W. Fang, T. F. T. Cerqueira, A. Sanna, M. A. L. Marques, and I. Errea, Ambient pressure high temperature superconductivity in RbPH_3 facilitated by ionic anharmonicity, arXiv [10.48550/arXiv.2411.03822](https://arxiv.org/abs/10.48550/arXiv.2411.03822) (2024).

Supplementary Information for: The Maximum T_c of Conventional Superconductors at Ambient Pressure

Kun Gao,¹ Tiago F. T. Cerqueira,² Antonio Sanna,³ Yue-Wen Fang,⁴ Đorđe Dangić,^{4,5}
Ion Errea,^{4,5,6} Hai-Chen Wang,¹ Silvana Botti,¹ and Miguel A. L. Marques^{1,*}

¹*Research Center Future Energy Materials and Systems of the University Alliance Ruhr and Interdisciplinary Centre for Advanced Materials Simulation, Ruhr University Bochum, Universitätsstraße 150, D-44801 Bochum, Germany*

²*CFisUC, Department of Physics, University of Coimbra, Rua Larga, 3004-516 Coimbra, Portugal*

³*Max-Planck-Institut für Mikrostrukturphysik, Weinberg 2, D-06120 Halle, Germany*

⁴*Centro de Física de Materiales (CFM-MPC), CSIC-UPV/EHU, Manuel de Lardizabal Pasealekua 5, 20018 Donostia/San Sebastián, Spain*

⁵*Fisika Aplikatua Saila, University of the Basque Country (UPV/EHU), Europa Plaza 1, 20018 Donostia/San Sebastián, Spain*

⁶*Donostia International Physics Center (DIPC), Manuel de Lardizabal Pasealekua 4, 20018 Donostia/San Sebastián, Spain*
(Dated: February 25, 2025)

* miguel.marques@rub.de

#1: Tl_2AgH_2

```

mat id agm002924843
  spg 139
  nsites 5
  e above hull 0.124 eV
  e form 0.101 eV
  decomposition Tl, Ag,  $\text{TlH}_4$ 
  ecutwfc 100.0 Ry
  kpts coarse  $16 \times 16 \times 16$ 
  kpts fine  $32 \times 32 \times 32$ 
  qpts  $4 \times 4 \times 4$ 
   $\lambda$  1.128
   $\omega_{\text{log}}$  141 K
   $\omega_2$  475 K
   $T_c^{\text{McMillan}}$  11.7 K
   $T_c^{\text{Allen-Dynes}}$  12.7 K
   $T_c^{\text{Eliashberg}}$  13.2 K

```

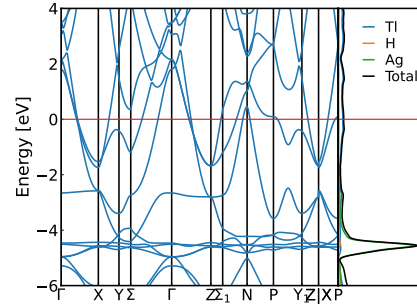
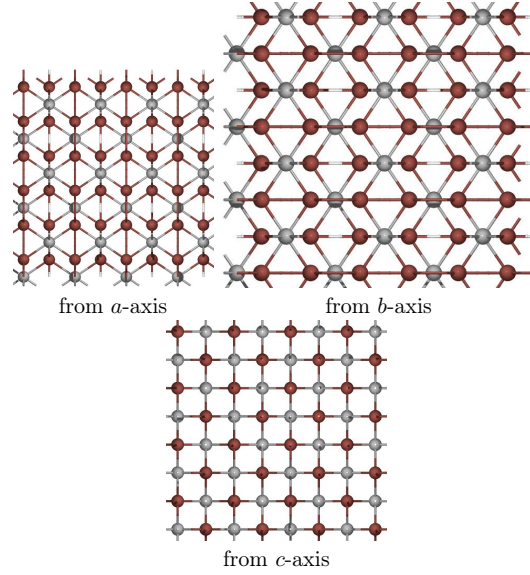
Primitive structure:

a : 5.0017 Å, b : 5.0017 Å, c : 5.0017 Å
 α : 118.36°, β : 118.36°, γ : 92.87°

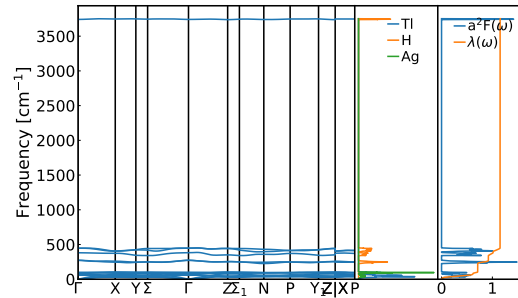
```

Tl [0.7500, 0.2500, 0.5000]
Tl [0.2500, 0.7500, 0.5000]
Ag [0.0000, 0.0000, 0.0000]
H [0.5555, 0.5555, 0.0000]
H [0.4445, 0.4445, 0.0000]

```



Electron band structure



Phonon band structure

#2: NaNiH₃

```

mat id agm002490730
  spg 221
  nsites 5
e above hull 0.014 eV
e form -0.241 eV
decomposition NaNiH3
ecutwfc 116.0 Ry
kpts coarse 16×16×16
kpts fine 32×32×32
qpts 4×4×4
  λ 0.158
  ωlog 1090 K
  ω2 1420 K
  TcMcMillan 0.0 K
  TcAllen-Dynes 0.0 K
  TcEliashberg 0.0 K

```

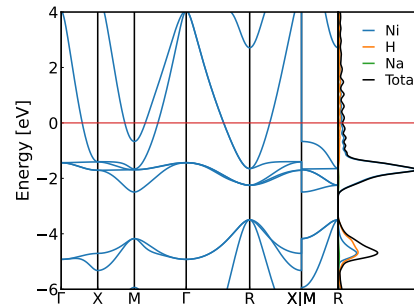
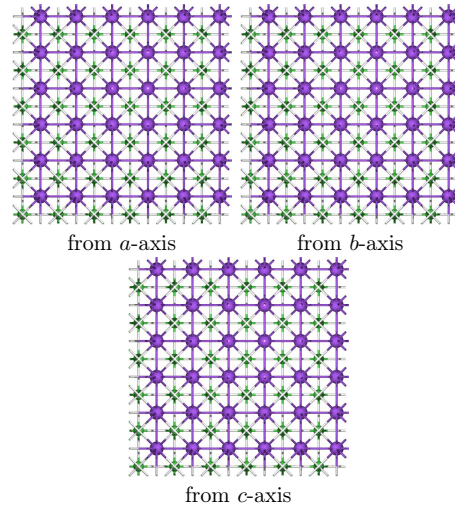
Primitive structure:

a : 3.3957 Å, b : 3.3957 Å, c : 3.3957 Å
 α : 90.00°, β : 90.00°, γ : 90.00°

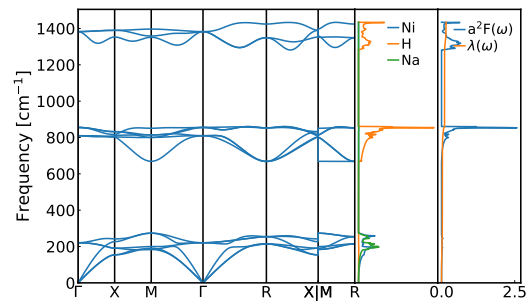
```

Na [0.5000, 0.5000, 0.5000]
Ni [0.0000, 0.0000, 0.0000]
H  [0.0000, 0.5000, 0.0000]
H  [0.0000, 0.0000, 0.5000]
H  [0.5000, 0.0000, 0.0000]

```



Electron band structure



Phonon band structure

#3: BC₁₁

```

mat id agm006148322
  spg 21
  nsites 12
e above hull 0.225 eV
e form 0.214 eV
decomposition C,B4C
ecutwfc 90.0 Ry
kpts coarse 12×12×16
kpts fine 24×24×32
qpts 3×3×4
  λ 0.551
  ωlog 1193 K
  ω2 1269 K
  TMcMillanc 20.7 K
  TAllen-Dynesc 21.2 K
  TEliashbergc 24.0 K

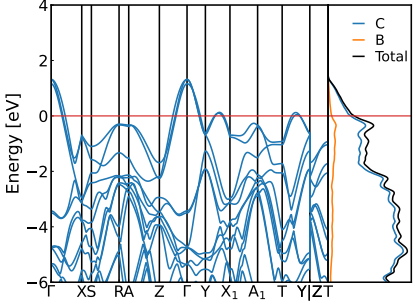
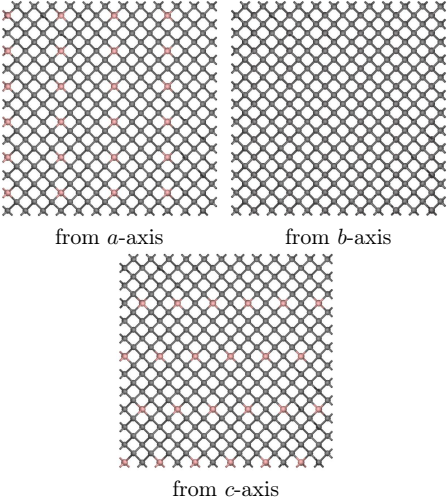
```

Primitive structure:
a: 5.7150 Å, *b*: 5.7150 Å, *c*: 3.5998 Å
 α: 90.00°, β: 90.00°, γ: 143.32°

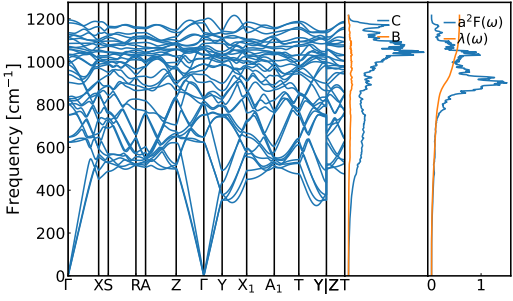
```

B [0.0000, 1.0000, 0.5000]
C [0.1696, 0.3409, 0.7555]
C [0.3332, 0.6668, 0.5000]
C [0.5000, 1.0000, 0.7471]
C [0.1673, 0.8327, 0.0000]
C [0.3409, 0.1696, 0.2445]
C [0.6668, 0.3332, 0.5000]
C [0.8304, 0.6591, 0.7555]
C [0.5000, 0.5000, 0.0000]
C [0.6591, 0.8304, 0.2445]
C [0.8327, 0.1673, 0.0000]
C [0.0000, 0.5000, 0.2529]

```



Electron band structure



Phonon band structure

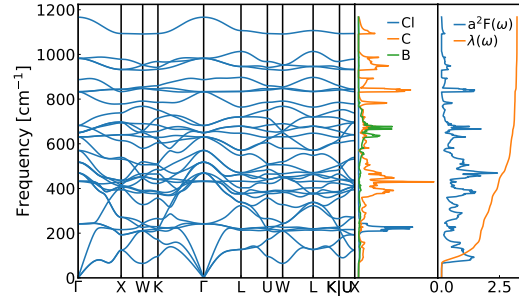
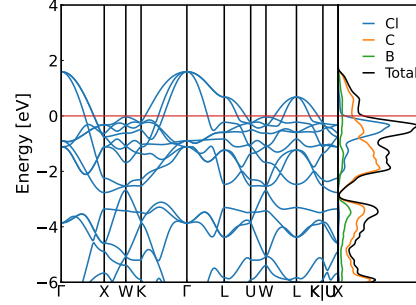
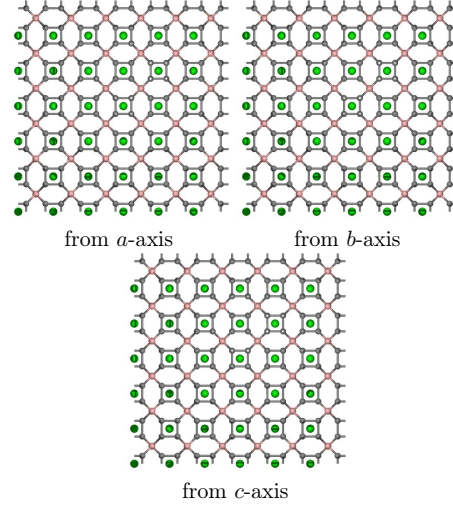
#4: B₂C₈Cl

mat id agm029547244
 spg 225
 nsites 11
 e above hull 0.989 eV
 e form 0.798 eV
 decomposition B₄C, BCl₃, C
 ecutwfc 90.0 Ry
 kpts coarse 12×12×12
 kpts fine 24×24×24
 qpts 3×3×3
 λ 3.278
 ω_{log} 294 K
 ω₂ 492 K
 T_c^{McMillan} 55.0 K
 T_c^{Allen-Dynes} 82.7 K
 T_c^{Eliashberg} 96.1 K

Primitive structure:

a: 4.9498 Å, *b*: 4.9498 Å, *c*: 4.9498 Å
 α: 60.00°, β: 60.00°, γ: 60.00°

B [0.2500, 0.2500, 0.2500]
 B [0.7500, 0.7500, 0.7500]
 C [0.8879, 0.3364, 0.8879]
 C [0.1121, 0.6636, 0.1121]
 C [0.8879, 0.8879, 0.8879]
 C [0.1121, 0.1121, 0.1121]
 C [0.3364, 0.8879, 0.8879]
 C [0.6636, 0.1121, 0.1121]
 C [0.8879, 0.8879, 0.3364]
 C [0.1121, 0.1121, 0.6636]
 Cl [0.5000, 0.5000, 0.5000]



#5: $\text{Al}_2\text{H}_7\text{Os}$

```

mat id agm006206343
  spg 225
  nsites 10
  e above hull 0.265 eV
  e form 0.097 eV
  decomposition Al2Os, H2
  ecutwfc 86.0 Ry
  kpts coarse 12×12×12
  kpts fine 24×24×24
  qpts 3×3×3
  λ 3.175
  ωlog 204 K
  ω2 596 K
  TcMcMillan 37.6 K
  TcAllen-Dynes 57.3 K
  TcEliashberg 100.0 K

```

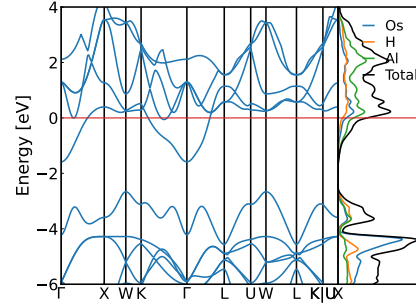
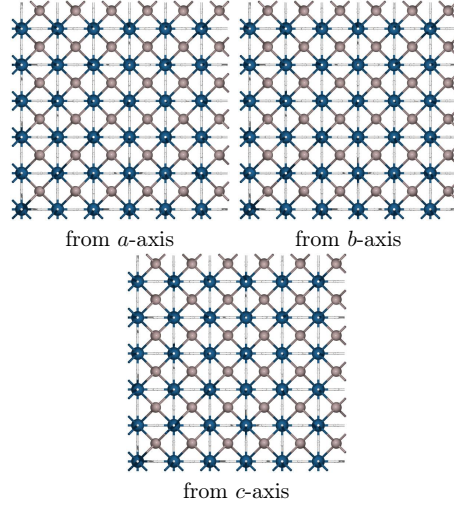
Primitive structure:

a : 4.5896 Å, b : 4.5896 Å, c : 4.5896 Å
 α : 60.00°, β : 60.00°, γ : 60.00°

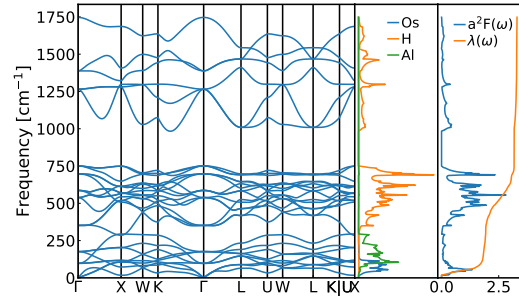
```

Al [0.7500, 0.7500, 0.7500]
Al [0.2500, 0.2500, 0.2500]
H [0.5000, 0.5000, 0.5000]
H [0.2721, 0.2721, 0.7279]
H [0.2721, 0.7279, 0.2721]
H [0.7279, 0.2721, 0.7279]
H [0.2721, 0.7279, 0.7279]
H [0.7279, 0.2721, 0.2721]
H [0.7279, 0.7279, 0.2721]
Os [0.0000, 0.0000, 0.0000]

```



Electron band structure



Phonon band structure

#6: Li_2AgH_6

```

mat id agm006188332
  spg 225
  nsites 9
e above hull 0.319 eV
e form 0.094 eV
decomposition LiH9, Ag, LiH
ecutwfc 104.0 Ry
kpts coarse 12×12×12
kpts fine 24×24×24
qpts 3×3×3
  λ 3.783
  ωlog 338 K
  ω2 655 K
  TcMcMillan 66.5 K
  TcAllen-Dynes 110.6 K
  TcEliashberg 132.3 K

```

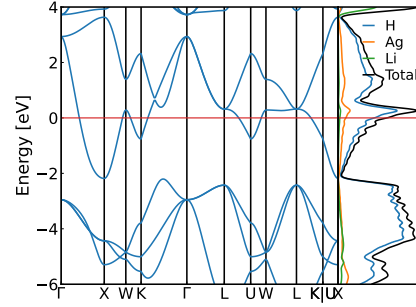
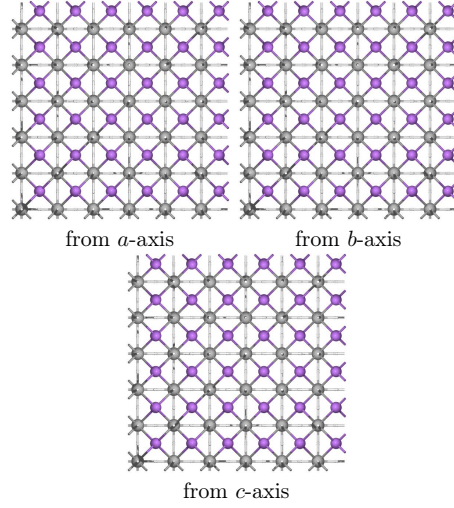
Primitive structure:

a : 4.6213 Å, b : 4.6213 Å, c : 4.6213 Å
 α : 60.00°, β : 60.00°, γ : 60.00°

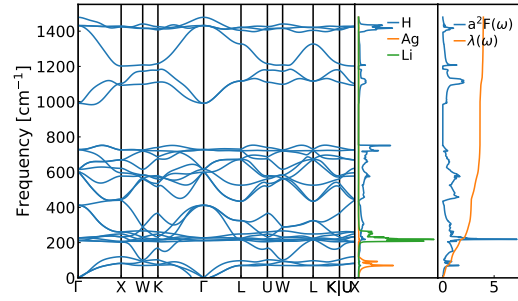
```

Li [0.7500, 0.7500, 0.7500]
Li [0.2500, 0.2500, 0.2500]
Ag [0.0000, 0.0000, 0.0000]
H [0.2654, 0.2654, 0.7346]
H [0.2654, 0.7346, 0.2654]
H [0.7346, 0.2654, 0.7346]
H [0.7346, 0.7346, 0.2654]
H [0.2654, 0.7346, 0.7346]
H [0.7346, 0.2654, 0.2654]

```



Electron band structure



Phonon band structure

To address the anharmonic phonon properties of Li_2AgH_6 and Li_2AuH_6 at ambient pressure, we used the stochastic self-consistent harmonic approximation (SSCHA) method [1–4]. In the case of Li_2AgH_6 , a $4 \times 4 \times 4$ supercell including 576 atoms was used in SSCHA calculations, which corresponds to the dynamical matrices on a commensurate $4 \times 4 \times 4$ \mathbf{q} -mesh. All the degrees of freedom were fully relaxed in the SSCHA calculations. Due to the heavy DFT calculations and the demanding number of structure configurations used for the convergence of Hessian phonons, we trained a Gaussian approximation potential [5] based on the DFT calculations. The converged free energy Hessian phonons were obtained by using the Gaussian approximation potential. In the anharmonic phonon calculations of Li_2AuH_6 , we employed $2 \times 2 \times 2$ supercell with 72 atoms that is sufficient to get convergence. The cutoff energy was 80 Ry with $10 \times 10 \times 10$ \mathbf{k} -point grid for the supercell calculations. We also performed electron-phonon coupling calculations for the anharmonic structure of Li_2AuH_6 , on $6 \times 6 \times 6$ \mathbf{q} -point grid with coarse \mathbf{k} -point sampling of $24 \times 24 \times 24$ and dense grid of $42 \times 42 \times 42$. The double delta sum was done with 0.004 Ry Gaussian smearing. The results are summarized in Table S1.

TABLE S1. Calculated electron-phonon coupling constant, ω_{log} , ω_2 , and T_c for Li_2AuH_6 . The superconducting critical temperature is calculated with McMillan’s formula and Allen-Dynes modified formula (AD) with $\mu^* = 0.1$, with harmonic phonons and anharmonic phonons from the SSCHA auxiliary force constants and those from the SSCHA free energy Hessian.

$\mu^* = 0.1$	Harmonic	Auxiliary	Hessian
λ	3.86	2.10	2.67
ω_{log} (K)	317	572	503
ω_2 (K)	724	982	870
T_c (K) - McMillan	63	85	86
T_c (K) - AD	108	107	118

Fig. S1 shows the comparison between the harmonic phonons from DFPT, anharmonic free energy Hessian phonon spectra, and the anharmonic auxiliary phonon spectra for both Li_2AgH_6 and Li_2AuH_6 .

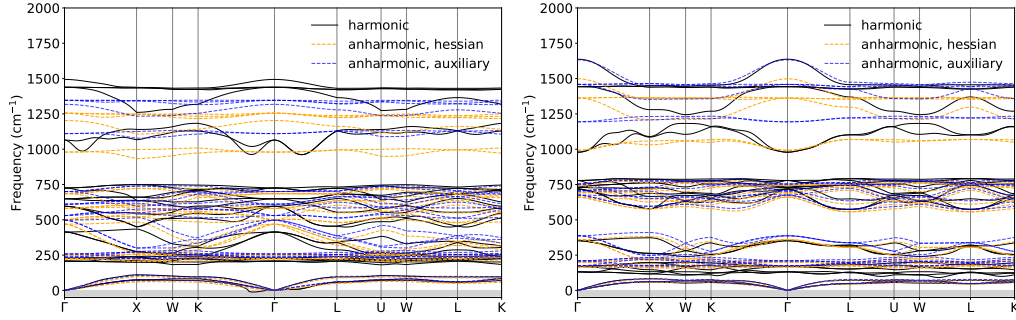


FIG. S1. Anharmonic free energy Hessian phonon spectra and anharmonic auxiliary phonon spectra of Li_2AgH_6 (left panel) and Li_2AuH_6 (right panel) calculated by the stochastic self-consistent harmonic approximation (SSCHA) at ambient pressure (the reader is referred to Refs. [2, 4] for details). The results are compared to the harmonic result. In the case of Li_2AgH_6 anharmonicity lifts the instability observed close to Γ in the harmonic case.

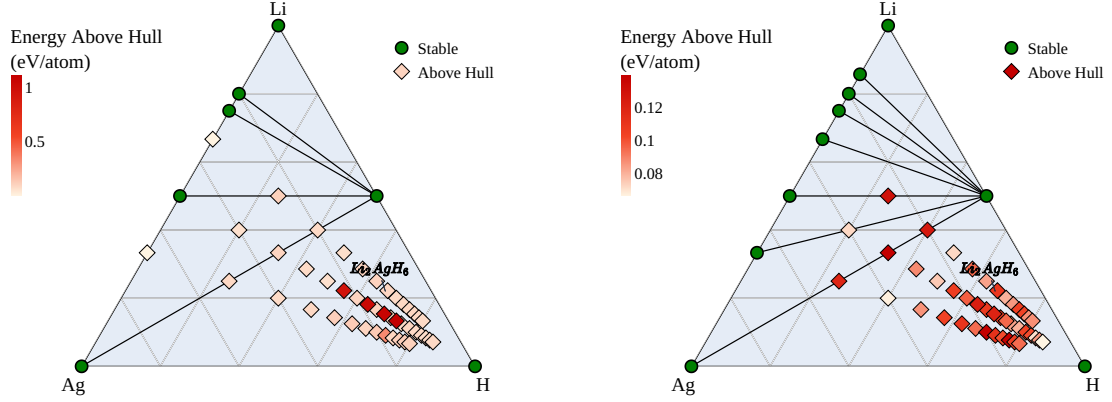


FIG. S2. The convex hull of the Li–Ag–H system at 25 GPa (left) and 50 GPa (right). Circles represent thermodynamically stable structures, and diamonds represent metastable structures.

-
- [1] Errea, I., Calandra, M. & Mauri, F. Anharmonic free energies and phonon dispersions from the stochastic self-consistent harmonic approximation: Application to platinum and palladium hydrides. *Phys. Rev. B* **89**, 064302 (2014). URL <https://link.aps.org/doi/10.1103/PhysRevB.89.064302>.
 - [2] Bianco, R., Errea, I., Paulatto, L., Calandra, M. & Mauri, F. Second-order structural phase transitions, free energy curvature, and temperature-dependent anharmonic phonons in the self-consistent harmonic approximation: Theory and stochastic implementation. *Phys. Rev. B* **96**, 014111 (2017). URL <https://link.aps.org/doi/10.1103/PhysRevB.96.014111>.
 - [3] Monacelli, L., Errea, I., Calandra, M. & Mauri, F. Pressure and stress tensor of complex anharmonic crystals within the stochastic self-consistent harmonic approximation. *Phys. Rev. B* **98**, 024106 (2018). URL <https://link.aps.org/doi/10.1103/PhysRevB.98.024106>.
 - [4] Monacelli, L. *et al.* The stochastic self-consistent harmonic approximation: calculating vibrational properties of materials with full quantum and anharmonic effects. *J. Phys. Condens. Matter*. **33**, 363001 (2021). URL <https://doi.org/10.1088/1361-648x/ac066b>.
 - [5] Bartók, A. P., Payne, M. C., Kondor, R. & Csányi, G. Gaussian approximation potentials: The accuracy of quantum mechanics, without the electrons. *Phys. Rev. Lett.* **104**, 136403 (2010). URL <https://link.aps.org/doi/10.1103/PhysRevLett.104.136403>.